Preparation and Preliminary Study of Structure-Controlled S2 Columnar Ice

Olivier Plé* and Jacques Meyssonnier*

Laboratoire de Glaciologie et Géophysique de l'Environnement du CNRS, associé à l'Université Joseph Fourier-Grenoble I, Rue Molière, BP96, 38402 Saint Martin d'Hères Cedex, France

Received: October 11, 1996; In Final Form: February 26, 1997[⊗]

The conical shape of the grains found in natural columnar S2 ice, or in "usual" S2 ice grown in the laboratory by simulating the natural seeding conditions, enhances boundary sliding in the direction parallel to the column axes. A process to grow a structure-controlled columnar ice that exhibits homogeneous grain diameter and cylindrical grains, the *c*-axis orientation of which can be controlled, is described. Brick-shaped specimens of "structure-controlled" and "usual" columnar ice, with their largest facets cut perpendicular to the long axis of the grains, have been tested under uniaxial constant compressive stress. The comparison of the results shows the interest of using "structure-controlled" columnar ice, which can be more easily modeled by two-dimensional analysis, under appropriate loading conditions, for fundamental studies of the deformation mechanisms in ice.

Introduction

Mechanical testing of S2 columnar ice aims at a better understanding of the mechanisms involved in the ice damage process that occurs during the interaction between a floating ice sheet and an offshore structure. In the laboratory, S2 columnar ice is usually grown from a primary layer of sieved snow crystals, by freezing water in a uniaxial vertical temperature gradient. The resulting grains are column shaped, with their long direction parallel to the direction of growth. As ice grows slower along the *c*-axis direction (hexagonal symmetry axis) than perpendicular to it,[1] well-oriented grains develop faster. Since the seeding crystals are oriented at random, this selection process favors the growth of grains with horizontal *c*-axes, at the expense of the others, which tend to disappear, and the final structure is actually that of imbricated cones, with grain *c*-axes approximately coplanar and randomly oriented in the plane perpendicular to the long direction of the columns. Its specific structure leads one to consider columnar ice as a macroscopically transversely isotropic material. Weeks and Ackley[2] observed that the mean diameter $\langle d \rangle$ of sea-ice columnar grains increases linearly with depth h, according to $\langle d \rangle = \langle d_0 \rangle + 0.033h$, where $\langle d_0 \rangle$ is the mean diameter of the grains at the surface. We made similar measurements on columnar ice grown in the laboratory from deionized pure water following the usual procedure as described by Gold,[3] Gold et al.,[4] Nixon and Wasif,[5] Sinha,[6] and Smith and Schulson.[7] The variation of $\langle d \rangle$ versus depth for pure "usual" ice was found as $\langle d \rangle = \langle d_0 \rangle + 0.047h$, for $0 < h < 100$ mm. The measurements were made by video-image processing to obtain the number of grains in a given area and then the average grain diameter. We observed that 80−90% of the initial number of grains had disappeared at 100 mm depth (this is in accordance with Weeks and Ackley's results[2]). As the measure of the grain mean diameter is made by considering both growing and disappearing grains, the above relations for $\langle d \rangle$ cannot give any reliable information on the conical shape of the grains. To estimate the variation of the grain shape versus depth, the increase in the diameter d_g of the growing grains was measured on thin sections cut perpendicularly to the columns. The relation for the mean value of d_g was found as $\langle d_g \rangle = \langle d_0 \rangle + 0.06h$ for $h > 35$ mm. But the evolution of the conical shape of the grains, very pronounced for the small diameters, is better represented by $\langle \mathrm{d}d_g/\mathrm{d}h \rangle = 2.3/h$, where h is in millimeters.

Deformation Mechanisms in S2 Columnar Ice

In the ductile range, the ice Ih single crystal deforms essentially by dislocation glide on the basal plane normal to the *c*-axis and then exhibits a very strong plastic anisotropy. According to Duval et al.,[8] the nonbasal deformation requires stresses at least 60 times larger than that for an easy-glide oriented crystal under the same strain rate at −10 °C. According to Kamb,[9] when a single crystal of ice deforms by simultaneous gliding along its three *a*-axes, following a power law with exponent n, the resultant gliding direction is exactly the same as that of the resolved shear stress on the basal plane if n is 1 or 3; for $1 < n < 3$, the maximum deviation is only on the order of 2°. Consequently the viscoplastic behavior of the ice single crystal may be considered as transversely isotropic. The elastic anisotropy is less marked, with a difference less than 10% in the Young's moduli along the *c*-axis direction and the direction perpendicular to it.[10]

These two types of anisotropy of the single crystal lead to strain incompatibilities in the ice polycrystal and are responsible for the development of an internal stress field that is nonuniform at the grain scale. According to Liu et al.,[11] grain boundaries can act as dislocation sources, because strain inhomogeneity between grains promotes grain boundary sliding, then stress concentrations at grain boundary facet intersections, and also as obstacles to the intracrystalline motion of dislocations, which results in dislocation pileups. Uniaxial and biaxial mechanical tests performed on natural or laboratory grown samples under constant stress or constant strain rate[3,6,12,13] confirm the nonlinear viscoplastic behavior of S2 columnar ice. Under loads applied in the plane perpendicular to the long direction of the columns, the strain rate follows a power law with a value of exponent n close to that found for equiaxed ice (glacier ice or T1 snow ice), in the stress range 0.1-1 MPa, and for temperatures between −40 and −10 °C.

Owing to its very strong anisotropy, the viscoplastic deformation of the single crystal can be considered as two dimensional when the single crystal is loaded in a plane exactly perpendicular to its basal planes. This plane strain assumption could be extended to the behavior of a columnar S2 ice polycrystal loaded

[⊗] Abstract published in *Advance ACS Abstracts,* June 1, 1997.

S1089-5647(96)03256-7 CCC: $14.00

perpendicularly to the column axes, if there were no relative displacement of the grains along their long direction. This would simplify the study of the influence of the local microstructure on the deformation mechanisms. Unfortunately the *c*-axes of natural S2 ice, or of laboratory grown S2 ice prepared in the usual way, are not exactly coplanar and may be inclined from 5° to 30° with respect to the plane perpendicular to the long direction of the columns.[3] Moreover, the conical shape of the grains enhances boundary sliding in the direction parallel to the column axes.[14] The crystallographic misorientation and the grain geometry may change the deformation processes occurring at the grain scale, as they offer a supplemental degree of freedom along the long direction of the columns, then increase the energy dissipation, and modify the local stress concentrations.

"Structure-Controlled" Ice Preparation and Growth

To remedy the defects of columnar ice grown by simulating the natural seeding conditions, we designed a process to grow "structure-controlled" columnar ice with cylindrical grains of controlled *c*-axis orientation. This type of ice will be referred to as "SC" ice in the following.

This ice is grown from a seeding polycrystalline plate which is built grain by grain. Each seeding grain is machined with a milling machine from a *c*-axis oriented single crystal and is given the shape of a prism with a hexagonal basis, such that the *c*-axis is perpendicular to the geometrical symmetry axis. The mean diameter of the seeding grains can be varied from 5 to 60 mm (the smallest size is limited by the milling process). Then the prisms are stuck together on a metallic plate, using deionized pure water. During this stage, the *c*-axes of the grains are controlled so that they lie in a plane parallel to the metallic plate (this positioning is achieved by using cross polarizers, to within ±5°) and so that each grain may be given a specific orientation. Then the surface of the seed plate is machined and polished in order to eliminate the excess of refrozen water. At the end of this stage, the seed plate is approximately 1 cm thick. All these operations are performed in a cold room at −15 °C.

The metallic plate with the seed grains is then completed with insulated sides to form a tank and placed in a cold room at 0 °C. After 6 h the polycrystalline seed is covered with deionized pure water at 0 °C, and the tank is placed on a freezing table, the temperature of which is adjusted in order to control the heat flux at the ice−water interface. Doing so, the growth of the polycrystal takes place in the vertical direction, from the bottom to the top of the tank. A speed-controlled agitator is immersed at the top of the tank in order to sweep the ice−water interface from air bubbles.

Owing to the hexagonal shape of the initial seeding crystals, which corresponds to the equilibrium configuration of triple junctions (grain boundaries at an angle of 120°[15]), grain boundary energy is not influential on the grain selection process that takes place during the growth of columnar ice. This process is then essentially controlled by the thermal transfers at the ice−water interface. According to Hobbs[1] and Fletcher,[16] the thermal conductivity of ice is about 5% greater parallel to the *c*-axis than perpendicular to it. Since all the *c*-axes of the seeding crystals are practically perpendicular to the direction of growth, the temperature gradient in the ice, at the ice−water interface, may be considered as independent of the position (i.e. the same for each grain). Moreover, the thermal conductivity anisotropy should lead to favoring vertical *c*-axis oriented crystals, which is not generally observed. The essential factor for the selective growth of the grains is that, owing to the structure of ice, growth parallel to the *c*-axis needs to bond a group of four water molecules to the crystal, whereas growth perpendicular to the *c*-axis needs only to bond a group two molecules;[1] then, for given temperature conditions at the interface, the growth velocity is much higher perpendicular to the *c*-axis than parallel to it. According to Hobbs,[1] selective growth between two adjacent grains (at growth velocity of 10^{-6} to 10^{-5} ms^{-1}) is then a function of their *c*-axis orientations relative to the grain boundary and the ice−water interface (Ketcham and Hobbs' rules[1]) and results from the equilibrium of the surface tension forces at the grain boundary, which becomes asymmetrical. Our observations have shown that, when the temperature of the metallic bottom of the ice tank was fixed, which implies that the heat flux conducted through the ice was decreasing since in this case the ice thickness increases versus time t as $t^{1/2}$ [17] and then that the mean growth velocity decreases as $t^{-1/2}$, the selective growth of the best oriented grain remained active even for initially well oriented seeding grains. The selection process can be slowed down by keeping the grain boundaries off-equilibrium; this can be achieved by increasing the driving force for solidification,

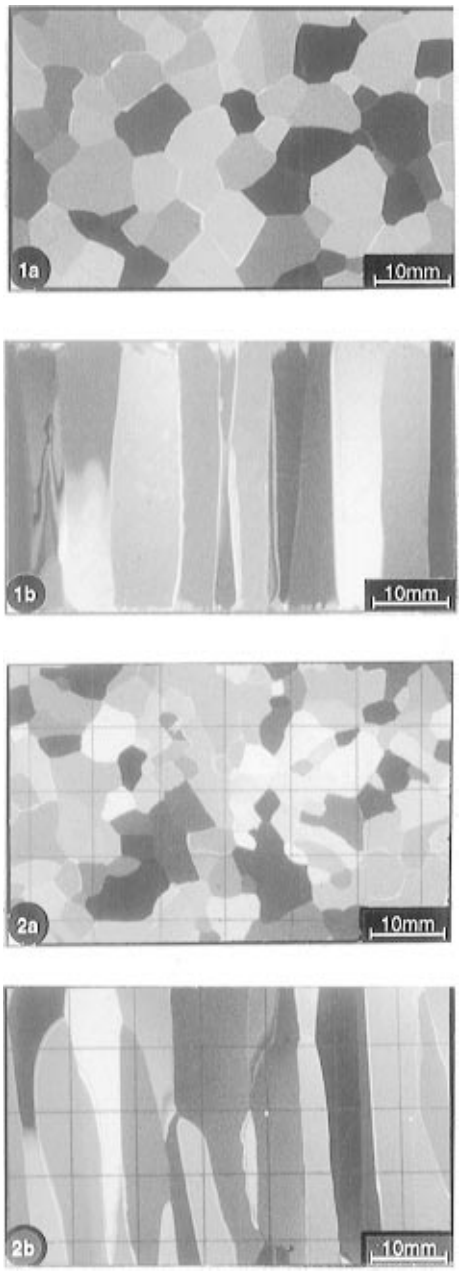

Figure 1. Photographs of thin sections, (a) across and (b) along the columns, of S2 columnar ice taken between cross polarizers: (1) "SC" ice; (2) "usual" ice.

that is, the heat flux extracted through the ice. In practice, the temperature of the freezing table, which can be varied from 0 to −42 °C, is adjusted so that the heat flux extracted at the ice−water interface is a constant;[18] it is then possible to obtain a polycrystalline plate up to 17 cm thick, with cylindrical grains. Contrary to "usual" ice, there are no disappearing grains, or newly nucleated grains, so that the average conicity $\langle \mathrm{d}d_g/\mathrm{d}h \rangle$ can be considered as negligible. The comparison between the structure of columnar ice grown in the usual way and that of our "SC" ice is shown in Figure 1. The resulting "SC" columnar ice exhibits homogeneous grain size (grain diameter in a section perpendicular to the long direction of the columns) and cylindrical grains with predetermined *c*-axis orientations.

Creep Test Experimental Procedure

Specimens of "SC" and "usual" columnar ice have been tested under uniaxial compression. The "usual" columnar ice was prepared by filling an open top and side-isolated tank, placed in a cold room at −10 °C, with deionized water. The ice film that formed at the water surface was removed, and the surface was covered with sieved ice crystals less than 0.5 mm in diameter, so that the ice plate was grown from the top to the bottom of the tank.

Brick-shaped specimens of "SC" and "usual" columnar ice were cut from the ice blocks using a band saw. The first upper 3 cm of the "usual" ice, which exhibited large variations in grain size and *c*-axis orientations, was discarded. For "SC" ice, the first lower 2 cm was kept aside in order to save the original seed polycrystal. Then the specimens were given the dimensions 260 × 130 × 50 mm, the largest facet being cut perpendicular to the long axis of the grains. They were machined carefully, by using a milling machine, in order to achieve good parallelism and perpendicularity of the facets, to within less than 0.15 mm. After machining, they were wrapped in sealing plastic film to avoid sublimation and then stored at −10 °C in the mechanical test dedicated cold room, for at least 24 h prior to testing.

A constant load was applied through steel plates, perpendicularly to the column axes, on the 130 × 50 mm ends. The upper platen of the press is connected to a fixed axial rod by a spherical articulation; the lower platen is fastened to the piston of a large diameter hydraulic jack; the constant loading pressure is obtained by connecting it to a small diameter and long stroke jack, the piston of which is pulled by weights. The specimens were accurately positioned on the lower platen by using four micrometer gauges to prevent a deviation of the loading axis from the specimen symmetry axis. The axial force was measured by means of a load cell mounted on the upper axial rod of the press. The axial strain ϵ_1, as well as the strain component ϵ_2 in the direction perpendicular to the loading axis and to the long direction of the columns, was recorded by means of LVDT extensometers, the legs of which were frozen directly on the specimen 70 mm apart. The strain component ϵ_3 in the direction perpendicular to the loading axis and along the columns was obtained by measuring the relative displacement of two vertical plastic sticks, 10 cm long, mounted on the ends of two LVDTs and placed on each side of the specimen. In addition, in order to estimate the relative displacement of the grains along their long axis direction, profiles of the specimen's largest facets along lines parallel to the loading direction were measured before and after each test, by using LVDTs mounted on the milling machine bench.

Creep Test Preliminary Results

Preliminary creep tests under uniaxial compressive stresses of 0.44 and 0.54 MPa were performed on three "usual" (grain diameter 5 ± 1.8, 6 ± 1.7, 9 ± 1.3 mm) and two "SC" (grain diameter 7.2 ± 0.3, 16.2 ± 0.5 mm) columnar ice specimens. All the tests were performed at the same temperature of −10 °C. The load was applied in the plane perpendicular to the long direction of the columns, along the long direction of the specimens, for 28 000 s (the deviation from test to test was less than 1%) and then removed. After unloading, the strain measurements were continued for more than 15 h.

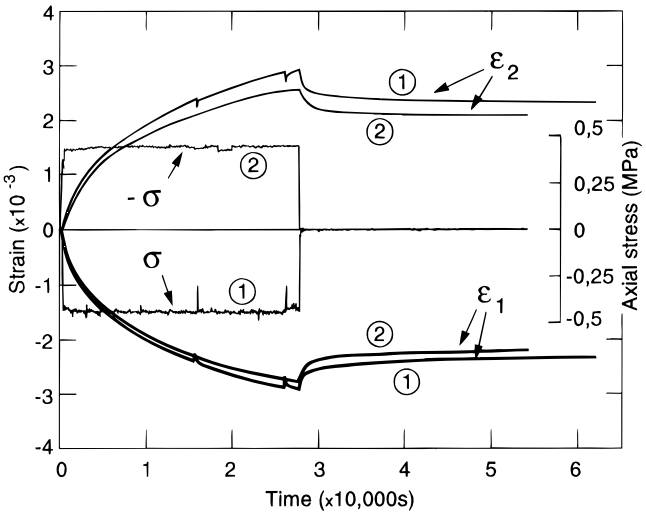

Figure 2. Axial ϵ_1 and transverse (across columns) ϵ_2 strains for "SC" and "usual" S2 columnar ice tested under uniaxial compression $\sigma = -0.44$ MPa, at −10 °C: (1) "SC" ice, grain diameter 7.2 mm; (2) "usual" ice, grain diameter 5 mm (the curve $-\sigma$ is drawn for clarity).

TABLE 1: Axial Strain ϵ_1^{max} and Strain Rate $\dot{\epsilon}_1^{u}$ Observed at $t = 28\,000$ s, and Recovered Strain ϵ_1^{rec} after 15 h, for the Different Tests

nature of ice	σ (MPa)	d (mm)	ϵ_1^{max} ($\times 10^{-3}$)	$\dot{\epsilon}_1^{u}$ ($\times 10^{-8}$)	ϵ_1^{rec} ($\times 10^{-4}$)
usual	−0.54	6.2 ± 1.6	−3.50	−4	8.4
usual	−0.53	9.2 ± 1.2	−3.56	−3.5	8.1
usual	−0.44	5.1 ± 1.8	−2.86	−2	6.0
SC	−0.44	16.2 ± 0.5	−3.19	−4	7.4
SC	−0.43	7.2 ± 0.3	−2.95	−3	4.8

An assessment of the strain measurement accuracy is given by the trace of the strain tensor measured at the end of each test. In the following, positive values of the strain correspond to elongation, negative values to shortening. Assuming that the strain recovery process is completed 15 h after unloading, the measured strains are theoretically the result of pure viscoplastic deformation and the sum $\epsilon_v^{\infty} = \epsilon_1 + \epsilon_2 + \epsilon_3$ should be zero. For "usual" as well as "SC" columnar ice, ϵ_v^{∞} was between 1×10^{-5} and 3×10^{-5} (positive values of ϵ_v^{∞} correspond to dilatation).

The greatest values of the total strain components were obtained just before unloading (at time $t \approx 28\,000$ s). The axial strain ϵ_1^{max} was in the range -2.8×10^{-3} to -3.5×10^{-3}, and the steady state was not reached (see Table 1 and Figure 2). At the same time the measured maximum values of ϵ_3 (along column strain) varied from 1.3×10^{-4} to 2.6×10^{-4} for "usual" columnar ice and from 5.7×10^{-5} to 6.5×10^{-5} for "SC" ice, i.e. 2−4 times less (see Figure 3). The analysis of the vertical profiles measured on the specimens showed that the geometry of "usual" ice was very distorted, even for the relatively small axial strain achieved in these tests: for some specimens the relative displacement of the grains along the direction of the column axes could reach 0.5 mm, and the final shape of the 250 × 50 mm section suggested the occurrence of buckling. Profiles measured on "SC" ice were much more even, with

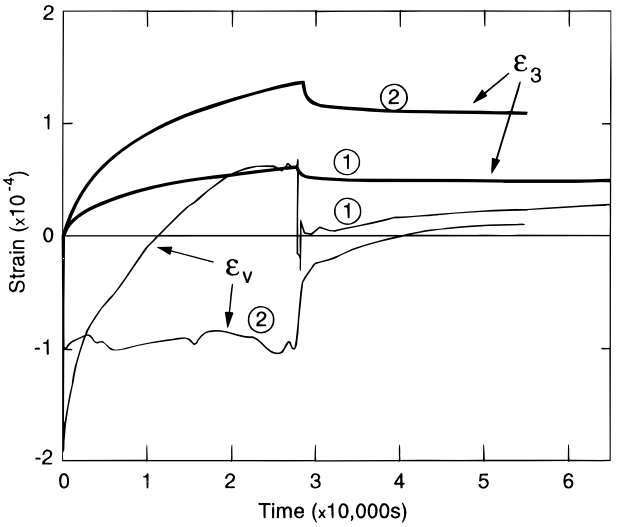

Figure 3. Along columns ϵ_3 and volumetric ϵ_v strains for (1) "SC" and (2) "usual" S2 columnar ice tested under uniaxial compression (test conditions given in Figure 2).

relative displacements less than 0.1 mm (i.e. on the order of the specimen machining accuracy). These observations lead one to consider that the plane strain assumption is more satisfactory for "SC" ice rather than for "usual" ice.

For all the tests, the axial strain rate $|\dot{\epsilon}_1|$ and the $\dot{\epsilon}_2$ component (in the plane perpendicular to the column axes) were very close to each other (see Figure 2). The $\dot{\epsilon}_3$ component was about 1 order of magnitude less for "usual" ice, and $\dot{\epsilon}_3$ for "SC" ice was between 2 and 4 times less than for "usual" ice (see Figure 3). Contrary to the $\dot{\epsilon}_3$ strain rate component, the absolute values of $\dot{\epsilon}_1$ and $\dot{\epsilon}_2$ for "SC" ice were always greater than for "usual" ice, and just before unloading the corresponding strain rates for "SC" ice were about twice that of "usual" ice at the same stress level (see Table 1). Assuming Glen's law under the form $\dot{\epsilon}_1 = A\sigma^3$, the strain rate at unloading can be fitted with $A = 2.5 \times 10^{-7}$ MPa^{-3} s^{-1} for "usual" ice and $A = 4.3 \times 10^{-7}$ MPa^{-3} s^{-1} for "SC" ice (Sinha's value[10] for "usual" ice is $A = 1.76 \times 10^{-7}$ MPa^{-3} s^{-1} at -10 °C).

Denoting by ϵ^{max} and ϵ^{∞} the total strain measured just before unloading and 15 h after unloading, respectively, and ϵ^e being an estimate of the purely elastic strain (computed with Sinha's data[10] for Young modulus $E \approx 9500$ MPa and Poisson ratio $\nu = 0.3$), the strain recovery computed as $\epsilon^{rec} = -(\epsilon^{max} - \epsilon^{\infty} - \epsilon^e)$ was greater for "usual" ice than for "SC" ice. The values of ϵ_1^{rec} are given in Table 1. For all the tests $|\epsilon_2^{rec}|$ was less than ϵ_1^{rec}. For "usual" ice $|\epsilon_3^{rec}|$ was on the order of 2×10^{-5} and was negligible for "SC" ice ($|\epsilon_3^{rec}| \approx 10^{-6}$, which is not significant). Contrary to Sinha's results,[6,19] we did not observe any significant influence of the grain size on strain recovery (a similar result for equiaxed T1 ice was noted by Meyssonnier and Goubert[20]).

The comparison of the strain rate components for "usual" and "SC" ice suggests that strain hardening proceeds more slowly for "SC" ice than for "usual" ice. The same result was obtained when fitting the axial strain curves for the first 100 s of 13 tests (8 of which were performed without measuring ϵ_3) with Andrade's law of the form $\epsilon_1 = -at^{1/3}$ (see Table 2). This can be explained by the fact that grain boundary sliding along the direction of the columns (enhanced by the conical shape of the grains) and the more marked misorientation of the *c*-axes in "usual" columnar ice provide an additional degree of freedom for the viscoplastic deformation in the direction of the columns; the corresponding increase in the dislocation density is accompanied by directional strain hardening, but also by a dislocation−dislocation interaction, which enhances strain hardening in the plane perpendicular to the column axes.

TABLE 2: Parameter *a* of Andrade's Law as a Function of the Applied Stress σ and Grain Diameter *d* (Fitted during the First 100 s of Each Test)

nature of ice	σ (MPa)	*d* (mm)	*a* ($\times 10^{-5}$ s$^{-1/3}$)
usual	−0.56	17 ± 3.1	3.04
usual	−0.53	9.2 ± 1.2	5.27
usual	−0.54	6.2 ± 1.6	5.63
usual	−0.41	9.8 ± 3.4	2.05
usual	−0.39	9 ± 1.3	2.21
usual	−0.42	6 ± 2.1	5.72
usual	−0.44	5.1 ± 1.8	4.10
usual	−0.42	4 ± 1.5	2.57
SC	−0.56	21 ± 0.5	4.04
SC	−0.57	18 ± 0.6	3.90
SC	−0.44	16.2 ± 0.5	5.48
SC	−0.40	10.1 ± 0.6	4.67
SC	−0.43	7.2 ± 0.3	6.57

Conclusion

A process of growing "structure-controlled (SC)" columnar ice that exhibits regular cylindrical grains with a controlled *c*-axis orientation has been presented. A few constant stress creep tests have been performed on this type of ice as well as on columnar ice grown by following the usual procedure. The comparison of the results obtained with these two types of ice showed that when columnar ice is loaded perpendicular to the long direction of the columns, "SC" ice is more prone to justify the plane strain assumption (induced by the strong viscoplastic anisotropy of the ice single crystal). This comparison also gives some indication of the relative influence of *out-of-plane* grain boundary sliding during the loading and unloading phases. *Despite the restrictions that result from the preliminary nature of this small data base*, this shows the interest of using our "SC" columnar ice, which can be more easily modeled by two-dimensional analysis (under appropriate loading conditions), for fundamental studies of the processes involved in the deformation of ice.

Acknowledgment. The technical help of O. Brissaud, J. Ph. Balestrieri, and A. Manouvrier was greatly appreciated. We wish to thank Drs. P. Duval and A. Philip, as well as an anonymous referee, for helpful comments and discussions.

References and Notes

(1) Hobbs, P. V. *Ice Physics*, 1st ed.; Clarendon Press: Oxford, 1974.
(2) Weeks, W. F.; Ackley, S. F. *The Geophysics of Sea Ice*; Nato ASI Series, *B-146*; 1986; Chapter 1.
(3) Gold, L. W. *Phil. Mag.* **1972**, *A26* (2), 311.
(4) Gold, L. W.; Jones, S. J.; Slade, T. D. *IAHR 92 11th Int. Symp. Ice* **1992**, *1*, 200.
(5) Nixon, W. A.; Wasif, M. A. *IAHR 92 11th Int. Symp. Ice* **1992**, *2*, 1167.
(6) Sinha, N. K. *Exp. Mech.* **1978**, *18* (12), 464.
(7) Smith, T. R.; Schulson, E. M. *Acta Metall. Mater*. **1993**, *41* (1), 153.
(8) Duval, P.; Ashby, M. F.; Anderman, I. *J. Phys. Chem.* **1983**, *87*, 4066.
(9) Kamb W. B. *J. Glaciol.* **1961**, *3* (30), 1097.
(10) Sinha N. K. *Cold Reg. Sci. Technol*. **1989**, *17* (2), 127.
(11) Liu, F.; Baker, I.; Dudley M. *Phil. Mag.* **1995**, *A71* (1), 15.
(12) Schulson, E. M.; Nickolayev, O. Y. *J. Geophys. Res.* **1995**, *100* (B11), 22383.
(13) Sinha, N. K.; Zhan, C.; Evgin, E. *J. Offshore Mech. Arctic Eng.* **1995**, *117*, 283.
(14) Nickolayev, O. Y.; Schulson, E. M. *Phil. Mag. Lett.* **1995**, *72* (2), 93.

(15) Ashby, M. F.; Jones, D. R. H. *Matériaux, t.2: Microstructure et Mise en Oeuvre*, 1st ed.; Dunod: Paris, 1991.

(16) Fletcher, N. H. *The Chemical Physics of Ice*, 1st ed.; Cambridge University Press: Cambridge, 1970.

(17) Lliboutry, L. *Traité de Glaciologie, t.1: Glace Neige et Hydrologie Nivale*, 1st ed.; Masson: Paris, 1964.

(18) Let T denote the temperature in the ice, T_m the melting point, $h(t)$ the ice thickness at time t, and x an abscissa counted from the bottom of the ice tank ($x = 0$) to the ice−water interface ($x = h$). A solution of the heat equation that verifies $T = T_m$ at $x = h(t)$ and leads to a constant heat flux Φ at the freezing front is given by $T = T_m - (L/c)(\exp\{-c\Phi(x-h)/(\lambda L)\} - 1)$, with $h = \Phi t/(\rho L) + h(0)$, where λ is the thermal conductivity of ice, c its specific heat capacity, L the latent heat of fusion, and ρ the ice density. To achieve such a temperature profile in the growing ice, up to thickness of about 20 cm, Φ must be adjusted so that the temperature of the ice tank bottom $T(0,t)$ is in the range 231−271 K allowed by the freezing table capacity.

(19) Sinha, N. K. *Phil. Mag.* **1979**, *A40* (6), 825.

(20) Meyssonnier, J.; Goubert, A. *Ann. Glaciol.* **1994**, *19*, 55.